

# Identification of Atrial Fibrillation Biomarkers through Virtual Populations with Anatomical and Electrophysiological Variability

Giada S. Romitti, María Termenón-Rivas, Alejandro Liberos, Miguel Rodrigo

Computational Multiscale Simulation Lab (CoMMLab), Department of Computer Science and  
Department of Electronic Engineering, Universitat de València, València, Spain

## Abstract

*Atrial fibrillation (AF) is a growing global health concern, driving the need for personalized diagnostic and treatment strategies. Computational modeling enables precision medicine by integrating patient-specific anatomical and electrophysiological data. In this study, we simulated sinus rhythm and arrhythmic behavior in 20 bi-atrial virtual patients, performing 800 simulations across varying structural and electrical remodeling parameters and stimulus locations. Key markers of increased AF vulnerability included greater lateral atrial extent, longer Bachmann's bundle, and higher total activation time, each linked to up to a 20% rise in AF inducibility. Electrical remodeling significantly increased arrhythmic incidence compared to less remodeled substrates ( $50 \pm 19\%$  vs  $37 \pm 19\%$ ,  $p = 0.02$ ), while impaired tissue conductivity (reduced diffusion) further heightened susceptibility ( $54 \pm 14\%$  vs.  $37 \pm 16\%$ ,  $p < 0.001$ ). Although the effects of remodeling and diffusion changes on AF inducibility were consistent across both atria, stimuli applied in the LA resulted in higher inducibility. These results highlight that AF progression due to remodeling or conduction impairment leads to more arrhythmogenic substrates, independent of anatomical variability. These findings support the use of virtual cohorts to uncover predictive biomarkers and guide individualized AF therapies.*

## 1. Introduction

Atrial fibrillation (AF) cases have risen by more than 30% over the last twenty years, with expectations that this growth will continue in the foreseeable future [1]. Advances in computational methods, especially those utilizing virtual patient populations and digital twin technologies, are becoming increasingly valuable for improving diagnosis, assessing risk, and personalizing treatment plans [2]. Due to significant differences in how patients respond to treatment, identifying consistent anatomical and electrophysiological biomarkers is essential for developing customized approaches to managing AF.

To ensure broad applicability, it is necessary to reflect both anatomical and electrophysiological diversity within the patient population. Recent investigations have addressed this challenge by employing virtual cohorts that modify either the electrical behavior of the heart while keeping anatomy fixed, or vice versa. These efforts have advanced our understanding of therapeutic response [3-5], facilitated the identification of important modeling parameters [6, 7], and generated synthetic datasets suitable for machine learning applications [8].

In this study, we employ a virtual cohort of bi-atrial anatomical models to simulate both sinus rhythm and arrhythmic activity, incorporating realistic anatomical and electrophysiological inter-patient variability as observed in AF populations. The virtual simulations aim to uncover structural and electrical biomarkers associated with the initiation and persistence of AF. Rather than focusing on patient-specific modeling, the objective is to analyze cohort-level variability and its influence on AF dynamics. By doing so, we aim to identify key indicators of AF susceptibility and progression, ultimately supporting the development of more targeted and effective therapeutic strategies.

## 2. Material and Methods

### 2.1. Computational domains

In this study, a subset of 20 atrial geometries was selected from a larger dataset generated using Statistical Shape Modeling (SSM) techniques [6]. These geometries were chosen to reflect the anatomical variability of the full cohort, based on eight key measurements per atrium. These measurements were calculated as Euclidean distances between specific anatomical landmarks. These metrics were selected to span major anatomical axes and structures, maximizing geometric heterogeneity across the selected set and promoting representativeness of the full population [3]. For the left atrium (LA), seven landmarks were used: the midpoint between the right pulmonary veins (RPVs), the midpoint between the left atrial appendage (LAA) and left pulmonary veins (LPVs), the center of the

posterior wall, the top of the mitral valve (MV), the fossa ovalis (FO), the apex of the LAA, and the midpoint between the LAA and the MV. In the right atrium (RA), seven points were identified: the bases of the superior vena cava (SVC) and inferior vena cava (IVC), the FO, the lateral base and apex of the right atrial appendage (RAA), the upper part of the tricuspid valve (TV), and the midpoint between the venae cavae.

The eight primary anatomical descriptors (M1–M8) used to characterize variation were: M1, the distance from the SVC to the IVC; M2, from the FO to the lateral base of the RAA; M3, from the upper part of the TV to the midpoint between the venae cavae; M4, from the midpoint between the LAA and the LPVs to the midpoint of the RPVs; M5, from the center of the posterior wall to the top of the MV; M6, from the FO to the midpoint between the LAA and MV; M7, from the apex to the base of the RAA; and M8, from the apex of the LAA to the midpoint between the LAA and MV. In addition to these landmark-based distances, two further anatomical indices were included: the lateral atrial extent (LAE), given by the sum of the distances from the LAA to the FO and from the FO to the RAA; and the length of Bachmann’s bundle (BBL), corresponding to the span between its insertion points in the left and right atria. Figure 1A illustrates all the anatomical landmarks and their associated measurements, while Figure 1B presents the numerical values and distribution of these measurements across the selected geometries.

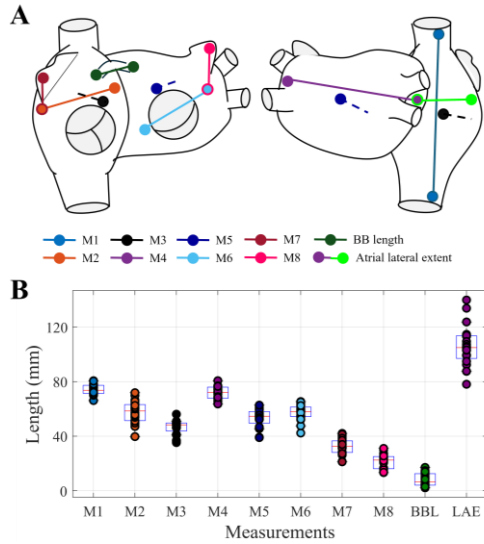


Figure 1. (A) Anatomical segments used for morphological measurements in the atrial geometries. (B) Measurements values distribution.

All geometries were remeshed into tetrahedral meshes at 0.5 mm resolution, yielding an average of  $644,240 \pm 75,155$  vertices and  $3,642,000 \pm 425,150$  elements. Fiber orientation, and tissue classification were assigned following the definitions from the original SSM dataset [6]

(Figure 2), while electrophysiological properties were assigned following previous literature [9].

## 2.2. Simulations framework

Atrial biophysical simulations were conducted using the Koivumäki et al. cellular model [10], in a monodomain model. In our simulations, two key changes were introduced to replicate AF-related substrate alterations: one affecting ionic remodeling and another affecting structural remodeling. Electrical remodeling was implemented by progressively altering the ionic properties of atrial cells, simulating the transition from a healthy state (0% remodeling;  $APD_{90}(2\text{ Hz})=240\text{ms}$ ) to a fully remodeled persistent AF state (100%;  $APD_{90}(2\text{ Hz})=102\text{ms}$ ), using intermediate levels of {50, 75, 100, 125}% remodeling [11].

In parallel, we modified the diffusion properties of the tissue to reflect structural remodeling. Diffusion governs the spread of electrical activation between neighboring cells and is influenced by both intercellular distances and tissue anisotropy. To simulate more advanced AF stages, global reductions in conduction were also introduced using scaling factors of 0.50 and 0.25, mimicking the effects of diffuse fibrotic remodeling on electrical propagation.

Simulations were executed using a custom GPU-accelerated finite element solver [12], with a temporal resolution of 20  $\mu\text{s}$ .

## 2.3. Simulated population

As illustrated in Figure 2, two types of simulations were conducted to explore atrial behavior under different physiological and pathological conditions. First, sinus rhythm simulations were performed on all 20 atrial geometries under baseline conditions (0% electrical remodeling and full diffusion (100%)) by applying a standard pacing protocol of five stimuli at 1000 ms intervals from the sinoatrial node (SAN). From these simulations, the total activation time (TACT) was computed as the difference between the local activation times of the last and first activated nodes.

To assess AF inducibility, additional simulations were carried out using decreasing pacing protocols applied at 10 different atrial sites (six in LA and four in RA, as shown in Figure 2). Each site was paced using a decreasing cycle length protocol (240 ms to 140 ms) across multiple substrate conditions, combining four levels of electrical remodeling (50%, 75%, 100%, and 125%) with two levels of reduced diffusion (25% and 50%).

To reduce computational cost, five of the ten stimulation sites were randomly selected for each substrate condition. AF was considered induced when self-sustained electrical activity persisted for at least five seconds following the final stimulus. In total, 800 simulations were performed,

corresponding to 20 virtual patients, 8 substrate combinations, and 5 pacing locations per condition.

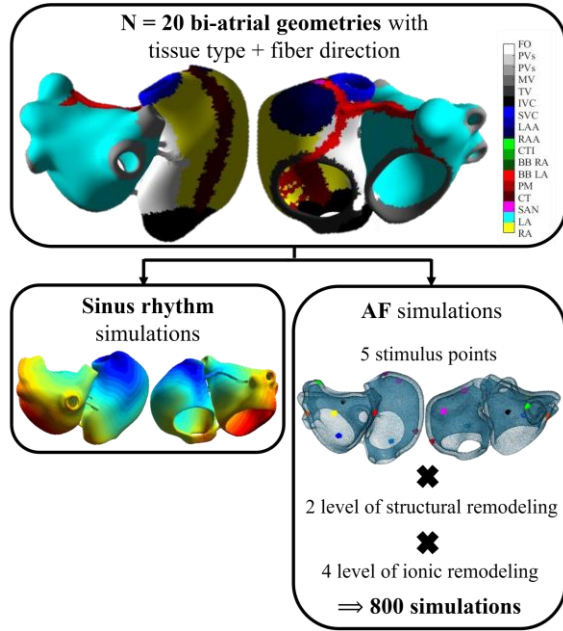


Figure 2. Simulation workflow.

### 3. Results

#### 3.1. Sinus Rhythm and Atrial Fibrillation induction

Simulations under sinus rhythm conditions (Figure 3A) produced local activation time (LAT) maps, with an average TACT of 120 ms, confirming the model's accuracy in capturing realistic electrophysiological behavior.

When inducing AF, models with AF substrates (25-50% diffusion  $\times$  50-125% remodeling) successfully maintained AF in 20-70% of the cases. Remodeling and diffusion changes had comparable effects on AF inducibility regardless of whether stimuli were applied in the LA or RA, although LA pacing sites consistently resulted in higher overall inducibility (Figure 3B)

We then explored the relationship between various parameters and arrhythmia occurrence. The effect of electrical remodeling on arrhythmia induction was evident, with substrates exhibiting more advanced remodeling showing a higher arrhythmic incidence ( $37 \pm 19\%$  vs  $50 \pm 19\%$ ,  $p = 0.02$ ). In addition, diffusion levels significantly influenced arrhythmia susceptibility, with lower diffusion rates leading to higher arrhythmic occurrences ( $54 \pm 14\%$  vs  $37 \pm 16\%$ ,  $p < 0.001$ ). These findings underline that advanced AF progression, whether due to electrical remodeling or decreased diffusion, promotes more arrhythmic substrates, irrespective of patient anatomy.

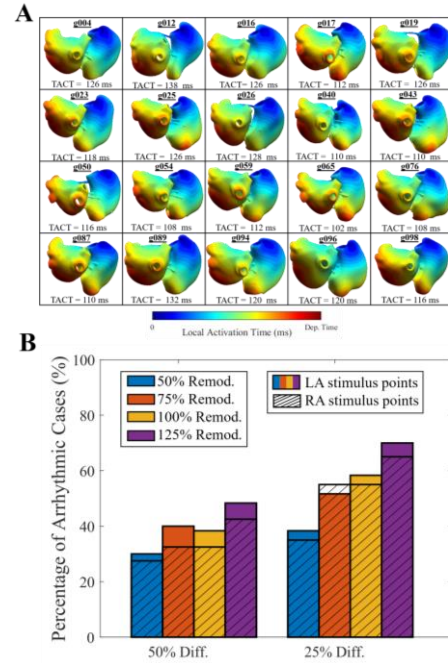


Figure 3. (A) LAT maps for each of the 20 atria included in the study, along with the TACT (in milliseconds) for each atrium. (B) Frequency of arrhythmic events observed across all combinations of ionic and structural remodeling, comparing the differences between stimulus points in the LA and RA.

#### 3.3. Anatomical and electrophysiological analysis of arrhythmicity

Arrhythmicity was analyzed in relation to patient-specific anatomical and electrophysiological parameters. Virtual patients with smaller lateral atrial extent ( $<105.8$  mm) showed lower arrhythmic inducibility ( $41 \pm 25\%$  vs  $51 \pm 22\%$ ,  $p = 0.01$ , Figure 4A), suggesting larger atria are more conducive to AF maintenance. Similarly, patients with larger Bachmann's bundle ( $>6.40$  mm) had higher arrhythmic rates ( $41 \pm 25\%$  vs  $49 \pm 22\%$ ,  $p = 0.02$ ). In terms of electrophysiology, patients with higher TACT ( $>118$  ms) also had higher AF incidence ( $40 \pm 24\%$  vs  $50 \pm 23\%$ ,  $p = 0.01$ , Figure 4B), indicating longer propagation times promotes AF persistence.

We then examined the effect of anatomical and electrophysiological parameters on AF progression. Patients with larger lateral atrial extent ( $>105.8$  mm) were more sensitive to electrical remodeling, with AF induction rates increasing from 31% to 53% for 50% and 125% remodeling, respectively (Figure 4C). In contrast, patients with smaller lateral extent showed a modest increase (26% to 38%) in AF incidence. A similar pattern was observed for sinus rhythm TACT: patients with shorter TACT ( $<118$  ms) exhibited less variation in AF inducibility (11%) compared to those with longer TACT (25%) (Figure 4D).

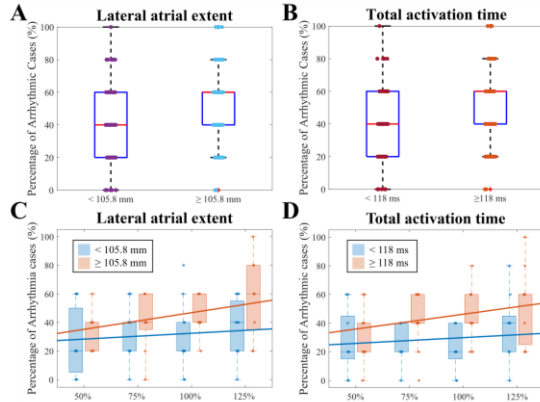


Figure 4. Total inducibility ratio as a function of: (A) Lateral atrial extent; (B) Total activation time. Inducibility ratio as a function remodeling for anatomies grouped by (C) atrial lateral extent and (D) total activation time.

#### 4. Discussion and Conclusions

This study examined a virtual cohort of 20 bi-atrial geometries across 800 simulations, varying electrical remodeling (APD) and diffusion (conductivity) to robustly assess AF inducibility. Consistent with expectations, greater remodeling and reduced diffusion increased arrhythmic vulnerability. Importantly, atrial anatomy, especially lateral extent, modulated susceptibility and its interaction with remodeling. Simulated TACT maps matched physiological sinus rhythm patterns, supporting the validity of our findings.

Prior studies have highlighted the need to account for both anatomical and electrophysiological variability in AF research to better guide therapy and ablation strategies. Our results reinforce this by showing that local anatomical features, such as lateral extent and activation time, modulate AF susceptibility in interaction with cellular remodeling. Unlike approaches based on total atrial volume [3], we selected geometries using inter-landmark distances to capture regional anatomical variation.

Although our sample includes only 20 bi-atrial geometries, future studies should expand cohort size and pacing coverage, as in [13], where over 200 stimulation sites were used to study arrhythmia vulnerability across fibrosis patterns.

This work's clinical relevance lies in using virtual cohorts to enhance patient-specific modeling and personalize AF treatment by identifying biomarkers of vulnerability and prognosis. Incorporating real-world measures like anatomical size or P-wave duration can further refine models, supporting efforts to prevent AF progression and improve clinical outcomes.

#### Acknowledgments

This work was funded by Generalitat Valenciana Grant

AICO/2021/318 (Consolidables 2021), Grants PID2020-114291RB-I00, PID2023-148702OB-I00 and EraNet PCI2024-153442 funded by MCIN/10.13039/501100011033 and by "ERDF A way of making Europe".

#### References

- [1] G. Lippi et al., "Global epidemiology of atrial fibrillation: an in-cresing epidemic and public health challenge," *International journal of stroke*, vol. 16, no. 2, pp. 217-221, 2021.
- [2] S. A. Niederer et al., "Creation and application of virtual patient cohorts of heart models," *Philosophical Transactions of the Royal Society A*, vol. 378, no. 2173, 2020.
- [3] A. Dasí et al., "In Silico TRIals guide optimal stratification of ATRial Fibrillation patients to Catheter Ablation and pharmacological medicaTION: the i-STRATIFICATION study," *Europace*, vol. 26, no. 6, euae150, 2024.
- [4] C. H. Roney et al., "Patient-specific simulations predict efficacy of ablation of interatrial connections for treatment of persistent atrial fibrillation," *EP Europace*, vol. 20, no. suppl\_3, pp. iii55-iii68, 2018.
- [5] P. M. Boyle et al., "Computationally guided personalized targeted ablation of persistent atrial fibrillation," *Nature biomedical engineering*, vol. 3, no. 11, pp. 870-879, 2019.
- [6] C. Nagel et al., C., "A bi-atrial statistical shape model for large-scale in silico studies of human atria: model development and application to ECG simulations," *Medical Image Analysis*, vol. 74, pp. 102210, 2021.
- [7] P. Martínez Díaz et al., "The right atrium affects in silico arrhythmia vulnerability in both atria," *Heart Rhythm*, vol. 21, no. 6, pp. 799-805, 2024.
- [8] C. H. Roney et al., "Predicting atrial fibrillation recurrence by combining population data and virtual cohorts of patient-specific left atrial models," *Circulation: Arrhythmia and Electrophysiology*, vol. 15, no. 2, pp. e010253, 2022.
- [9] J. Barrios-Álvarez de Arcaya et al., "Role of Fiber Direction and Ionic Heterogeneities in Atrial Arrhythmia Simulations," In *2023 Computing in Cardiology (CinC)*, vol. 50, pp. 1-4, 2023.
- [10] J. T. Koivumäki et al., "In silico screening of the key cellular remodeling targets in chronic atrial fibrillation," *PLoS Computational Biology*, vol. 10, no. 5, 2014.
- [11] G. S. Romitti et al., "Implementation of a Cellular Automaton for efficient simulations of atrial arrhythmias," *Medical Image Analysis*, pp. 103484, 2025.
- [12] V. García-Mollá et al., "Adaptive step ODE algorithms for the 3D simulation of electric heart activity with graphics processing units," *Computers in biology and medicine*, vol. 44, pp. 15-26, 2014.
- [13] L. Azzolin et al., "A reproducible protocol to assess arrhythmia vulnerability in silico: pacing at the end of the effective refractory period," *Frontiers in physiology*, vol. 12, 656411, 2021.

Address for correspondence:

Miguel Rodrigo Bort  
Av. de l'Universitat, s/n. 46100, Burjassot (Valencia, Spain).  
miguel.rodrigo@uv.es